Implications of Accelerated Recombination-Active Defect Complex Formation for Mitigating Carrier-Induced Degradation in Silicon

Brett J. Hallam, Malcolm D. Abbott, Nitin Nampalli, Phill G. Hamer, and Stuart R. Wenham

***Abstract*—A three-state model is used to explore the influence of the accelerated formation of recombination-active defect complexes on the mitigation of carrier-induced degradation in p-type silicon containing boron and oxygen. Defect formation is observed to be a critical factor for the speed at which carrier-induced degradation can be mitigated. Defect formation also plays a critical role in determining the effectiveness of mitigation at elevated temperatures. It is observed that under conventional conditions, at a processing temperature of 200 °C, approximately 170 s are required to form and passivate 99% of possible defects. The experimentally demonstrated improved effectiveness of carrier-induced defect passivation with a process time of 10 s at temperatures over 300 °C is consistent with a substantial acceleration of defect formation.**

***Index Terms*—Boron–oxygen (B–O), carrier-induced degradation (CID), Czochralski silicon, defect formation, hydrogen passivation, light-induced degradation (LID), regeneration.**

I. Introduction

CARRIER-INDUCED defects have presented themselves as a significant issue for silicon solar cells due to the fact that the recombination-active defects form under typical operating conditions for modules in the field [1], [2]. One such carrier-induced recombination-active defect in boron-doped Czochralski silicon, often referred to as a light-induced defect, has been attributed to a boron–oxygen (B-O) complex. It should be noted, however, that this B-O defect is not exclusive to Czochralski silicon. It is also found in other boron- and oxygen-containing silicon materials such as p-type multicrystalline silicon (although to a lesser extent due to reduced oxygen concentrations) [2]–[4].

The exact configuration and process of defect formation continues to be debated in the literature [2], [5]–[7]. Some models have suggested the recombination-active defect consisted of a substitutional boron (B_s) atom and an interstitial oxygen dimer (O_{2i}). In contrast, an alternative hypothesis has suggested the involvement of silicon self-interstitials (Si_i) rather than interstitial oxygen dimers (O_{2i}) in the defect complex [6]. At this point in time, the exact configuration still appears unclear. In this paper, we assume the defect is comprised of a B-O complex.

Similarly, many contradictory theories have been presented for the permanent deactivation of carrier-induced recombinati on-active defect complexes in boron-doped Czochralski silicon, as first demonstrated by Herguth *et al.* [8]. In particular, the involvement of hydrogen in the permanent deactivation process has been heavily debated. Numerous groups have noted the involvement of hydrogen in the process and the importance of hydrogen charge states [9]–[15]. However, the incorporation of hydrogen in many of these studies was done by plasma-based processes, which have been suggested to enhance hydrogen diffusivity [16]. This could also raise questions on whether the plasma exposure itself, in conjunction with thermal process used for fast-firing, enables the permanent recovery during subsequent illuminated annealing. Purely thermal-based understandings have also been proposed, attributed to Ostwald ripening of nanoprecipitates in the material [17], particularly during fast-firing processes [7]. However, in that study, permanent mitigation of carrier-induced degradation (CID) was only demonstrated in the samples containing hydrogen. A recent letter has provided strong evidence that the process is not purely thermal, or purely due to plasma exposure before fast-firing, and that hydrogen is likely involved in the process [18]. This is in agreement with many other independent research groups concluding that hydrogen is involved and that it is able to consistently explain the data in the literature [9]–[15]. Hence, in this paper, we attribute the permanent recovery to hydrogen passivation of the recombination-active defect complex.

A previous three-state model used to describe the system for the permanent deactivation of carrier-induced defects in boron-doped Czochralski silicon had focused on a modulation of the rates of permanent passivation reaction [19]. In particular, the emphasis was placed on the ratio of the reactions that, in this paper, are denoted as the defect passivation process, and the destabilization process, respectively. However, no consideration was given to the influence of variations in the defect formation rate.

In this paper, we explore the implications of accelerated defect formation on both the effectiveness and speed of mitigating CID in boron-doped Czochralski silicon. This is based on new insights, with an acceleration of defect formation in p-type silicon under high intensity illumination [20] that can enable the complete mitigation of CID on p-type Czochralski solar cells

Manuscript received May 31, 2015; revised September 21, 2015; accepted October 16, 2015. Date of publication November 19, 2015; date of current version December 18, 2015. This work was supported by the Australian Government through the Australian Renewable Energy Agency (ARENA). This work was also supported by the commercial partners of the ARENA 1-060 advanced hydrogenation project and the U.K. Institution of Engineering and Technology through the A. F. Harvey Engineering Prize. The views expressed herein are not necessarily the views of the Australian Government, and the Australian Government does not accept responsibility for any information or advice contained herein.

The authors are with the School of Photovoltaic and Renewable Energy Engineering, University of New South Wales, Kensington, N.S.W. 2052, Australia (e-mail: brett.hallam@unsw.edu.au; m.abbott@unsw.edu.au; nnampalli@gmail.com; phillhamer@gmail.com; stuartwenham@gmail.com).

Color versions of one or more of the figures in this paper are available online at http://ieeexplore.ieee.org.

Digital Object Identifier 10.1109/JPHOTOV.2015.2494691

with a standard full-area aluminum back-surface field within 8 s of being turned into a working device [21].

II. Dynamics of the Boron–Oxygen Defect Complex System

A. Defect Formation

Defect formation for CID in boron-doped Czochralski silicon has long been thought of as independent of carrier injection in p-type silicon solely doped with boron for illumination intensities above 0.01 suns [2]. This has been verified by numerous authors [22], [23] and was attributed to the role of electrons and, hence, Δn in enabling defect formation. Defect formation rates have been reported to depend on the equilibrium hole concentration (p_0), with increasing formation rates for increased p_0 values. However, increasing this value through an increase in boron doping, as has typically been done in the literature, also increases the saturation normalized defect concentration in the material when subjected to carrier injection [2]. Hence, for a given wafer, in such studies, the only dependence for defect formation rate at illumination intensities above 0.01 suns in p-type silicon was reported to be due to temperature.

Results presented by Hamer *et al.* have suggested a dependence of defect formation in p-type silicon on the total hole concentration (p) [20]. This was achieved through the use of high intensity illumination to drive the silicon material into high injection such that the excess hole concentration (Δp) leads to a significant increase in p. This suggested that the defect formation rate could be modulated by both temperature and carrier injection. As both temperature and carrier injection are used for the permanent deactivation process to passivate the B-O defect complex, changes to carrier injection in the permanent deactivation process could also change the defect formation rate.

It should be noted that while we assume the defect is a B-O complex, the actual structure and composition of the defect are not pivotal to the findings in this work.

B. Defect Passivation

In 2006, Herguth *et al.* presented a permanent deactivation process for eliminating CID in silicon containing boron and oxygen, through the use of illumination at elevated temperatures [8]. One possible theory for this permanent passivation reaction that is able to consistently explain the data in the literature is based on hydrogen [12], [14], [15], [24]–[28]. In this reaction, a recombination-inactive complex is formed, presumed to be a hydrogen-defect complex. Different kinetics and reaction time constants have been reported for different solar cell structures and different illumination intensities [28], [29]. This can be explained by differences in the total concentration of hydrogen, fractional hydrogen charge state concentrations, as well as changes to the fractional concentrations of the defect in the positive charge state [12], [14], [15], [24], [26]–[28].

It should be noted that while we assume the involvement of hydrogen and present the model in this context, the involvement of hydrogen is not pivotal to the key findings in this paper. The key findings are that effective and rapid mitigation through the passivation of the carrier-induced defects requires an acceleration of defect formation.

C. Destabilization and the Dissociation of Carrier-Induced Defects

Elevated temperatures can lead to the thermal dissociation of the carrier-induced defect, returning the silicon material into a recombination-inactive state. However, after dissociation, the carrier-induced defect can still form under subsequent illumination [30], [31]. Thermal dissociation rates of the defects are thought as independent of illumination intensity. Similarly, after the passivation of the B-O complexes, subsequent annealing at elevated temperatures can thermally dissociate the hydrogen-defect complex, in a process termed "destabilization." This typically occurs at temperatures above 200 °C. After destabilization, the defect can rapidly dissociate, returning the silicon into a recombination-inactive, although unstable state. In this paper, we assume that the thermal dissociation rates for the defect complex and the hydrogen-defect complex are only dependent on temperature.

III. Mathematical Model

A three-state model is used to describe the B–O complex system associated with CID in boron-doped Czochralski silicon, in a similar manner as has been used by Herguth and Hahn [19]. However, in this work, the model has been adapted based on more recent understandings with the involvement of hydrogen in the passivation process and the ability to accelerate defect formation. The first state (A) describes the silicon material after high-temperature processing before the formation of the recombination-active defect complex. Hence, state A is comprised of the dissociated defect constituents, which form the recombination-active defect complex under illumination.

The second state (B) describes the material in the degraded state after the formation of the carrier-induced defect complex. This typically occurs after exposure to carrier injection at relatively low temperatures.

The third state (C) describes the silicon material once the recombination-active defects have been passivated, to form a recombination-inactive hydrogen-defect complex. This is typically achieved after the injection of hydrogen into the silicon during fast-firing and a subsequent hydrogenation process incorporating minority carrier injection. State C is stable with exposure to subsequent minority carrier injection. It should be noted that at any given time, a mix of the states may be present in the silicon.

For the three-state model, six transitions are mathematically possible. However, not all of the transitions appear to have a physical relevance for the system. The transition from state A to state B (T_{AB}) describes the formation of the recombination-active defect complex under carrier injection. The reverse transition from state B to state A (T_{BA}) describes the thermal dissociation of the recombination-active defect complex. The transition from state B to state C (T_{BC}) describes the passivation of the recombination-active defect complex to form a recombination-inactive hydrogen-defect complex. The transition from state C to state B (T_{CB}) describes the destabilization

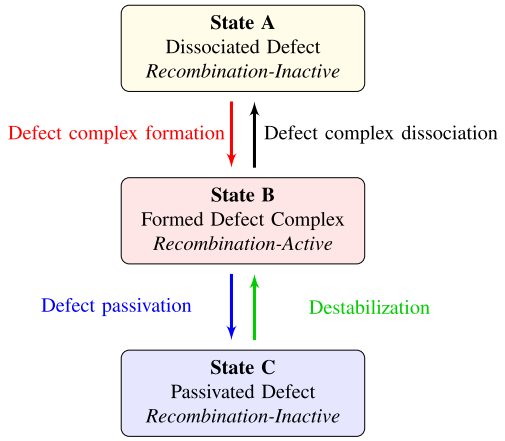

Fig. 1. Diagrammatic representation for the three-state model for B–O defect complex system associated with CID in boron-doped Czochralski silicon.

reaction with the thermal dissociation of the hydrogen-defect complex, back to a recombination-active defect complex that is isolated from hydrogen.

The transition from state C to state A (T_{CA}) does not appear feasible, as it would involve the complete dissociation of the hydrogen-defect complex simultaneously, including the dissociation of hydrogen from the defect, and the dissociation of the recombination-active defect complex. Furthermore, the reported attempt frequencies and activation energies for T_{CB} and T_{BA} as published in the literature result in a rate constant for T_{CB} more than two orders of magnitude lower than that of T_{BA}. Hence, if the hydrogen-defect complex dissociates to leave the hydrogen isolated from the defect, the defect is almost immediately thermally dissociated, therefore shifting the system back to state A. This means that if a sample with passivated B-O defects was destabilized at elevated temperatures, then as the system changes from having all defects in state C to having all defects in state A, no significant population of defects will build up in state B, and hence, no significant degradation would be measured experimentally. Similarly, the transition from state A to state C (T_{AC}) does not appear feasible. Hence, in this work, T_{AC} and T_{CA} will be ignored. A diagrammatic description of the three-state system is shown in Fig. 1.

For each reaction T_{ij}, there exists an activation energy ($E_{a,ij}$) from state i to state j and associated attempt frequency (v_{ij}). The activation energies and attempt frequencies are shown in Table I.

The normalized concentrations in each of the states ($N_i(t)$), where $i = \mathrm{A}, \mathrm{B}, \mathrm{C}$, are governed by a system of linear differential equations given by (1)–(3) below. Here, κ_{ij} is the rate constant from state i to state j according to the Arrhenius equation as shown in (4):

$$\frac{\delta N_A}{\delta t} = \kappa_{BA} \cdot N_B - \kappa_{AB} \cdot N_A \quad (1)$$

$$\frac{\delta N_B}{\delta t} = \kappa_{AB} \cdot N_A + \kappa_{CB} \cdot N_C - (\kappa_{BA} + \kappa_{BC})\, N_B \quad (2)$$

$$\frac{\delta N_C}{\delta t} = \kappa_{BC} \cdot N_B - \kappa_{CB} \cdot N_C \quad (3)$$

$$\kappa_{ij} = v_{ij} \cdot e^{\frac{-E_a}{k_b T}}. \quad (4)$$

TABLE I
ACTIVATION ENERGIES (E_a) AND ATTEMPT FREQUENCIES (v_{ij}) FOR TRANSITIONS FROM STATE i TO STATE j (T_{ij}) IN THE B–O DEFECT COMPLEX SYSTEM ASSOCIATED WITH CARRIER-INDUCED DEGRADATION IN BORON-DOPED CZOCHRALSKI SILICON

Process	T_{ij}	E_a (eV)	v_{ij} (1/s)	Ref.
Defect formation	T_{AB}	0.475	4×10^3	[32]
Defect dissociation	T_{BA}	1.32	1×10^{13}	[32]
Defect passivation	T_{BC}	0.98	1.25×10^{10}	[13]
Destabilization	T_{CB}	1.25	5×10^9	[13]

IV. INFLUENCE OF DEFECT FORMATION RATES ON THE AVAILABILITY OF DEFECTS FOR PASSIVATION

Defect formation rates greatly influence the time that is required to fully form the carrier-induced defects in a given material, in preparation for defect passivation. In a conventional degradation process operating in low injection in p-type silicon, only a very low illumination intensity is required of approximately 0.01 suns [2]. Above this illumination intensity, while still operating in low injection no further acceleration of defect formation rates have been observed. This is due to sufficient minority carriers being present to drive the reaction(s) involving electrons for defect formation, with a critical value for saturation reported of approximately $1 \times 10^{11}/\mathrm{cm}^3$ [22]. Subsequently, the defect formation rate is limited by the availability of holes, hence depending on p_0 [33]–[35]. To accelerate defect formation, material with a higher p_0 could be used; however, this also increases the saturated defect concentration, which is undesirable for solar cells.

In p-type material of typical doping densities for solar cell fabrication ($N_a \approx 1 \times 10^{16}/\mathrm{cm}^3$), thermally generated holes have little influence on p_0 in the typical temperature range used for defect formation. Furthermore, during defect formation, the expected defect concentrations are many orders of magnitude lower than p_0 ($\approx 1 \times 10^{11} - 1 \times 10^{13}/\mathrm{cm}^3$) [32], [36]. Hence, the capture of two holes for the formation of each defect has little influence on p, and the v_{AB} is not reduced [35], [37]. In contrast, in n-type silicon, in low-injection conditions, p is orders of magnitude lower than that in p-type silicon. This can explain the defect formation rates in n-type silicon being typically four to five orders of magnitude slower than that in p-type [33].

The attempt frequency for defect formation in p-type silicon with $p_0 = 1 \times 10^{16}/\mathrm{cm}^3$ has been reported as $v_{AB} = 4 \times 10^3/\mathrm{s}$ [32], suggesting that 99% of defects can form within 25 h at a temperature of 30 °C. To determine a lower limit on the time required to have a certain fraction of possible defects available for passivation within a hydrogen-based model, two assumptions can be made. First, the hydrogen-related reactions (T_{BC} and T_{CB}) are neglected. Second, it is assumed that no thermal dissociation of the defects occurs (T_{BA}). Fig. 2 shows the time required to form 99% of defects at different temperatures based for different attempt frequencies. Hence, using an attempt frequency of $v_{AB} = 4 \times 10^3/\mathrm{s}$, to have a process throughput time of 1 s for complete defect formation (99%), a temperature of more than 500 °C would be required. For a processing time of 10 s, a minimum temperature of 330 °C would be required just to have 99% of defects available for passivation.

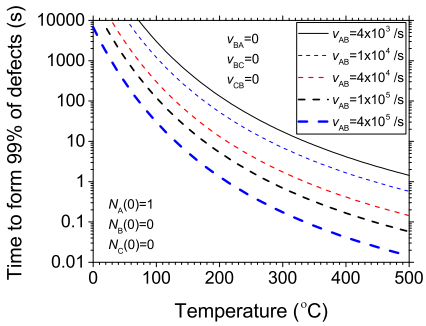

Fig. 2. Time required to form 99% of potential defects in boron-doped Czochralski silicon starting from a nondegraded state ($N_A = 1$), neglecting defect dissociation and hydrogen-related reactions ($v_{BA} = v_{BC} = v_{CB} = 0$). The reference case with $v_{AB} = 4 \times 10^3$/s represents boron-doped Czochralski silicon with an effective doping density of $N_a = 1 \times 10^{16}/\mathrm{cm}^3$ in low injection.

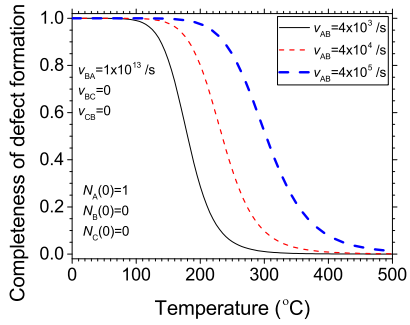

Fig. 3. Completeness of defect formation for different defect formation rates including the effects of defect dissociation ($v_{BA} = 1 \times 10^{13}$/s). All hydrogen-related reactions are ignored ($v_{BC} = v_{CB} = 0$). The reference case with $v_{AB} = 4 \times 10^3$/s represents boron-doped Czochralski silicon with an effective doping density of $N_a = 1 \times 10^{16}/\mathrm{cm}^3$ in low injection.)

TABLE II
RATIO OF THE TIME TAKEN TO FORM A GIVEN FRACTION x OF DEFECTS COMPARED WITH THAT REQUIRED TO FORM 99% OF AVAILABLE DEFECTS (λ_x), NEGLECTING THERMAL DISSOCIATION AND HYDROGEN-RELATED REACTIONS

x	0.50	0.80	0.90	0.95	0.98	0.99
λ_x	0.15	0.35	0.50	0.65	0.85	1.00

In contrast, by accelerating defect formation one order of magnitude ($v_{AB} = 4 \times 10^4$/s), a 1s process for complete defect formation could be realized at a temperature of approximately 330 °C, while a 21 °C process would allow complete defect formation within 10 s. This shifts closer to an industrial in-line process for the complete passivation of carrier-induced defects being realized. Further accelerations of the defect formation could further reduce the temperature requirements for defect formation and shorten the processing time.

The minimum time required to form a certain fraction of possible defects can simply be calculated as a ratio of the time to form 99% of defects, again ignoring defect dissociation. Table II shows typical ratios (λ_x) of the time to form a given fraction, (x) of defects compared with the time required to form 99% of defects [see (5)]. A change in the characteristic frequency for defect formation scales linearly with the reduction in time required. For example, a tenfold increase in characteristic frequency reduces the required time by a factor of 10:

$$\lambda_x = \frac{t_{B=x}}{t_{B=0.99}}. \tag{5}$$

.

V. INFLUENCE OF DEFECT FORMATION RATES ON THE COMPLETENESS OF DEFECT FORMATION

The dissociation of defects will act to reduce the instantaneous concentration of formed defects. Hence, defect dissociation will reduce the availability of defects for passivation. We now consider the case where the defect formation and defect dissociation processes are enabled, but still ignore hydrogen-related reactions (T_{BC} and T_{CB}). The time to reach steady state is also ignored.

The completeness of defect formation greatly depends on temperature. As the activation energy for defect dissociation is substantially larger than that of defect formation, a much greater temperature dependence is observed for the rate of defect dissociation than that for defect formation. Hence, while the defects can still effectively form in silicon at elevated temperatures, the competing dissociation process can almost immediately dissociate the formed defects. Fig. 3 shows the completeness of defect formation in steady state as a function of temperature for different defect formation rates. The point at which 50% of the population is in the degraded state ($N_B = 0.5$) and the other 50% of the population is in the dissociated state ($N_A = 0.5$) corresponds to the temperature at which the product of the defect formation rate (κ_{AB}) and the population in the dissociated state (N_A) is equal to the defect dissociation rate (κ_{BA}) and the population in the degraded state (N_A), i.e., $\kappa_{AB} \cdot N_A = \kappa_{BA} \cdot N_B$. For a conventional characteristic frequency $v_{AB} = 4 \times 10^3$/s, this corresponds to a temperature ($T_{N_B=0.5}$) of 180 °C. For temperatures above 230 °C, less than 10% of potential defects are formed at any given time.

While it is assumed that the defect dissociation rate is only dependent on temperature, the defect formation rate can be accelerated by using high intensity illumination [20]. Increasing the defect formation rate can shift the equilibrium fractional populations in the different states, such that higher concentrations of formed defects can be realized at higher temperatures. As shown in Fig. 3 increasing the defect formation rate by one order of magnitude can shift $T_{N_B=0.5}$ up to approximately 235 °C. Hence, with sufficient defect generation, completely degraded ($N_B > 99\%$) samples could be realized at substantially higher temperatures.

VI. INFLUENCE OF DEFECT FORMATION AND DEFECT DISSOCIATION ON CARRIER-INDUCED DEGRADATION MITIGATION

Time constants for the defect passivation reaction of approximately 3 s have been reported at 200 °C, suggesting that CID can be mitigated in less than 10 s [13]. However, this is only

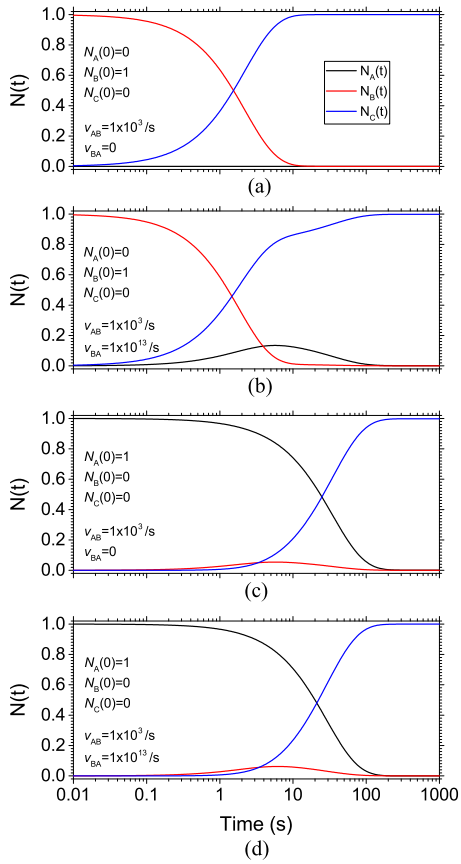

Fig. 4. Evolution of defect state population ($N_i(t)$) for the three states (state A = the dissociated state, state B = the formed defect complex state, state C = passivated state) on a sample processed at 200 °C for different scenarios. (a) Starting with all defects preformed ($N_B = 1$) and neglecting defect dissociation ($v_{BA} = 0$) or (b) including dissociation ($v_{BA} = 1 \times 10^{13}$/s). (c) Starting with all defects in the dissociated state ($N_A = 1$) and neglecting defect dissociation ($v_{BA} = 0$) or (d) including defect dissociation ($v_{BA} = 1 \times 10^{13}$/s). For all scenarios, an attempt frequency of $v_{AB} = 4 \times 10^3$/s is used for defect-complex formation (consistent for p-type silicon with $N_a = 1 \times 10^{16}/\mathrm{cm}^3$), $v_{BC} = 1.25 \times 10^{10}$/s is used for passivation, and $v_{CB} = 5 \times 10^9$/s for destabilization.

valid if, at all times, all defects are available for passivation. In reality, this is not the case, and therefore, the time to effectively passivate 99% of potential defects should depend on whether a given sample starts in a degraded state, or requires defect formation. The dissociation of the defects can further increase the time required to passivate the defects as it acts as a competing process to passivation. Furthermore, any dissociated defects will again require defect formation in order to be passivated.

In the same study reporting a 3-s time constant for the passivation process, it was experimentally demonstrated that it took approximately 30 s to passivate 99% of defects. This included several separate illuminated annealing processes (of several seconds duration), with a full 24-h degradation process performed in between each illuminated annealing process [13]. The intermediate degradation processes essentially made all defects available for passivation at the beginning of the subsequent illuminated annealing process. This time to mitigate CID is substantially longer than the reported time constant for defect passivation under the same illumination conditions and is, therefore, consistent with the hypothesis presented in this work that the time to mitigate CID depends on the availability of defects for passivation.

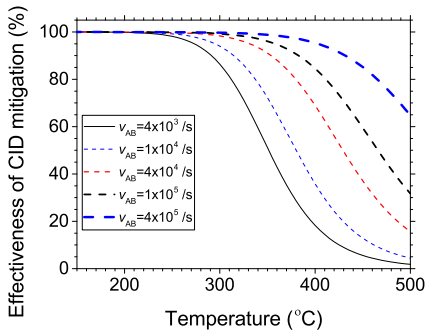

Fig. 5. Theoretical effectiveness of CID mitigation for different defect formation rates (v_{AB}). The effectiveness of CID mitigation is directly proportional to the fraction of the population of defects in the passivated state (N_C). For all scenarios, an attempt frequency of $v_{BA} = 1 \times 10^{13}$/s is used for defect dissociation, $v_{BC} = 1.25 \times 10^{10}$/s is used for passivation, and $v_{CB} = 5 \times 10^9$/s for destabilization.

Further evidence to support this hypothesis is demonstrated in Fig. 4, with theoretical simulations for the time required to passivate 99% of defects at 200 °C under different scenarios. As a best-case scenario for the time required to passivate the defects, a sample should start with all defects preformed, and no dissociation of the defects should occur. Under this regime, the time to achieve effective passivation only depends on the passivation and destabilization rates. Assuming the destabilization rate is only dependent on temperature, the time to achieve effective passivation of the defects is only dependent on the passivation rate. If a defect passivation rate of $v_{BC} = 1.25 \times 10^{10}$/s is also assumed, this suggests a minimum time of approximately 10 s if starting from a degraded state (neglecting defect dissociation). If allowing the dissociation of defects, approximately 110 s are required. Further increases in time are required if the sample also requires defect formation (140 s ignoring defect dissociation and 170 s including defect dissociation). The substantial difference in times required in the above scenarios suggests a strong dependence on the availability of the defects for passivation, and that in some instances, this may become the limiting factor. Hence, to accelerate the mitigation of CID, the defect formation rate should be increased.

VII. Implications of Accelerated Defect Formation on Mitigating Carrier-Induced Degradation at Elevated Temperatures

An acceleration of defect formation can also impact the effectiveness of CID mitigation at elevated temperatures. Fig. 5 shows theoretical predictions of the effectiveness of CID mitigation for different defect formation rates. The model indicates that simply by accelerating defect formation beyond the saturation rate imposed by using low-injection conditions ($v_{BA} = 4 \times 10^3$/s for boron-doped p-type silicon with $N_a = 1 \times 10^{16}/\mathrm{cm}^3$), the effectiveness of CID mitigation through hydrogenation can be improved. The use of increased temperatures has further benefits

in accelerating both the formation of the recombination-active defect complex and the passivation reaction.

Symmetrical lifetime test structures were fabricated using standard commercial grade 156 mm × 156 mm boron-doped Czochralski wafers (1.6 Ω · cm, $N_a = 9.1 \times 10^{15}/\mathrm{cm}^3$). Wafers were alkaline textured, with a resultant total wafer thickness of approximately 180 μm, followed by acidic neutralization, an RCA clean and HF dip. Phosphorus emitter diffusion was performed to achieve a sheet resistance of approximately 65 Ω/□ with a 30-min $POCl_3$ deposition at 795 °C followed by a drive-in for 40 min at 885 °C. Subsequently, a 75-nm-thick layer of hydrogenated silicon nitride (SiN_x : H) with a refractive index of 2.08 at 633 nm was deposited onto both surfaces of the wafers using a Roth & Rau MAiA plasma-enhanced chemical vapor deposition system. Wafers were fired in an inline belt furnace manufactured by SierraTherm using a firing profile with a peak temperature of approximately 620 °C. Dark annealing was performed on a hotplate with a wafer temperature of approximately 230 °C for 10 min prior to the laser process to ensure that B-O defects were not present in the samples.

A high illumination intensity laser process was applied to the wafers to accelerate defect formation [20] and passivate the formed defects. The process was performed on a hotplate under laser illumination using a 938-nm laser, operating in quasi-continuous wave mode with a pulse length of 0.5 ms and repetition frequency of 2 kHz. A homogenous illumination intensity of approximately 3.1×10^{19} photons/cm^2/s (145 suns) was used over the process region with a diameter of 4 cm. The temperature was measured in situ using a Calex PyroCouple PC301HT-0 infrared thermometer, with sensing radiation wavelengths of 8–14 μm. The output was logged using a USB-4704-AE high-speed logger, sampling at 100-ms intervals. The output voltage was then calibrated using a contact thermocouple without illumination. Temperatures reported are the equilibrium temperatures reached during the process. The process duration was 10 s with the wafers taking approximately 3–4 s to reach thermal steady state.

The stabilized lifetime values were measured after a 48-h light soak under a halogen lamp with a light intensity of 78 ± 1 mW/cm^2 with wafers maintained at a temperature of 308 ± 3 K. Control samples were also prepared with no attempt to passivate the B–O defects.

The normalized defect density, N_{DD}, can be measured on lifetime test structures to determine the effectiveness of CID mitigation. The N_{DD} is calculated using (6) [38], where τ_{eff} is the effective minority carrier lifetime, and $\tau_{\text{eff},DA}$ is the τ_{eff} of the sample after appropriate dark annealing (such as 10 min at 230 °C) to dissociate all B–O defects. The τ_{eff} values are measured using the generalized photoconductance technique[39], [40] on a Sinton Instruments WCT-120 tool at an excess carrier concentration $\Delta_n = 0.1 \times N_a$, where N_a is the acceptor doping concentration. Experimentally, the effectiveness of CID mitigation (CID_{mit}) is given by (7), where $N_{DD,\text{stabilized}}$ is the normalized defect density after the passivation process and subsequent light soaking to activate unpassivated B-O defects, and $N_{DD,\text{degraded}}$ is the normalized defect density after light soaking

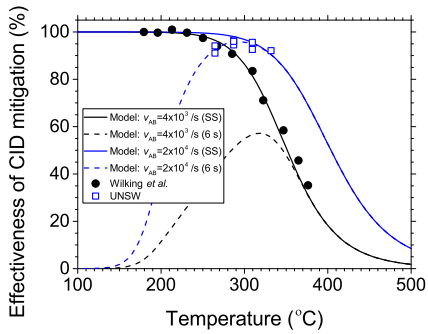

Fig. 6. Effectiveness of CID mitigation as reported by Wilking *et al.* [41] under steady-state conditions at 2.7-sun illumination and using data from UNSW using an illuminated annealing process of 10-s duration (approximately 6 s at the specified temperature) using an illumination intensity of approximately 145 suns. The theoretical effectiveness is shown for a conventional defect formation rate ($v_{AB} = 4 \times 10^3/\text{s}$) under steady-state conditions (SS) in close agreement with the data from Wilking *et al.* and a 6-s process. Simulations are also shown using an accelerated defect formation rate ($v_{AB} = 2 \times 10^4/\text{s}$) under steady-state conditions and a 6-s process consistent with the UNSW data. For all scenarios, an attempt frequency of $v_{BA} = 1 \times 10^{13}/\text{s}$ is used for defect dissociation, $v_{BC} = 1.25 \times 10^{10}/\text{s}$ is used for passivation, and $v_{CB} = 5 \times 10^9/\text{s}$ for destabilization.

with no attempt to passivate the B-O defects

$$N_{DD} = \frac{1}{\tau_{\text{eff}}} - \frac{1}{\tau_{\text{eff},DA}} \tag{6}$$

$$\text{CID}_{mit} = \frac{N_{DD,\text{stabilized}}}{N_{DD,\text{degraded}}}. \tag{7}$$

Experimentally, it has been observed that by increasing the illumination intensity, higher temperatures can be used to effectively mitigate CID in p-type Czochralski silicon [41]. To further validate the model used in this work, we also compared it with data from Wilking *et al.* Fig. 6 shows that the effectiveness of CID mitigation as presented by Wilking *et al.* using an illumination intensity of 2.7 suns in steady-state conditions is consistent with a defect formation rate of $v_{AB} = 4 \times 10^3/\text{s}$. The graph also highlights that by accelerating the defect formation rate (achieved through the use of high intensity illumination), a higher percentage of defects were stabilized at the elevated temperatures. A simulation of a 6-s process is also shown with an accelerated defect formation rate of $v_{AB} = 2 \times 10^4/\text{s}$ and this is found to be in agreement with the UNSW data. It should be noted that the reduced effectiveness of CID mitigation for temperatures below 290 °C is due to insufficient time to form and/or passivate the B-O defects. In previous work, the improved effectiveness of CID mitigation with increasing illumination intensity has been reported to be due to an acceleration of the permanent stabilization reaction (T_{BC}) [41]. In this work, we attribute the improved mitigation of CID at elevated temperatures to an acceleration of defect formation [20], although a simultaneous acceleration of the passivation process cannot be ruled out.

VIII. Conclusion

The formation and passivation rates of carrier-induced defects in p-type Czochralski were incorporated into a three-state

defect model to describe the mitigation of CID. The influence of defect formation and defect dissociation on the time to have the recombination-active defects available for passivation was shown, which can greatly influence the time taken to allow the mitigation of CID. Under conventional scenarios at a processing temperate of 200 °C using low-injection conditions with no acceleration of defect formation, on boron-doped silicon ($N_a = 1 \times 10^{16}/\mathrm{cm}^3$), approximately 170 s are theoretically required to form and passivate 99% of the defects.

The influence of defect formation rate on the effectiveness of CID mitigation at elevated temperatures was also explored. Empirical data presented by Wilking *et al.* using a light intensity of 2.7 suns were also compared, consistent with a generation of defects under conventional low-injection conditions that reduced the effectiveness of CID mitigation at temperatures over 230 °C. Using an illuminated annealing process developed at UNSW with increased illumination intensities (up to 145 suns), limitations of a reduced effectiveness of the passivation process at elevated temperatures as reported in previous studies have been overcome. In this work, we attribute the improved effectiveness at elevated temperatures to an acceleration of defect formation by operating the silicon samples cell under high-injection conditions, in agreement with numerical simulations assuming a defect formation rate of $v_{AB} = 2 \times 10^4/\mathrm{s}$.

ACKNOWLEDGMENT

The authors would like to thank D. Chen, M. Y. Kim, A. Azmi, and N. Gorman for the assistance with laboratory processing in this work.

REFERENCES

[1] H. Fischer and W. Pschunder, "Investigation of photon and thermal induced changes in silicon solar cells," in *Proc. 10th IEEE Photovoltaic Spec. Conf.*, 1973, pp. 404–411.

[2] J. Schmidt and K. Bothe, "Structure and transformation of the metastable boron- and oxygen-related defect center in crystalline silicon. *Phys. Rev. B*, vol. 69, art. no. 024107, Jan 2004.

[3] D. W. Cunningham, A. Parr, J. Posbic, and B. Poulin, "Performance comparison between bp solar mono and traditional multicrystalline modules," in *Proc. 23rd Eur. Photovoltaic Solar Energy Conf. Proc.*, Valencia, Spain, 2008, pp. 2829–2833.

[4] J. Schmidt, "Light-induced degradation in crystalline silicon solar cells," *Solid State Phenomena*, vol. 95, pp. 187–196, 2003.

[5] V. Voronkov, R. Falster, B. Lim, and J. Schmidt, "Boron-oxygen related lifetime degradation in p-type and n-type silicon," *J. Appl. Phys.*, vol. 50, no. 5, pp. 123–136, 2012.

[6] C. Möller and K. Lauer, "Light-induced degradation in indium-doped silicon," *Physica Status Solidi (RRL)–Rapid Res. Lett.*, vol. 7, no. 7, pp. 461–464, 2013.

[7] D. Walter *et al.*, "Effect of rapid thermal annealing on recombination centres in boron-doped Czochralski-grown silicon," *Appl. Phys. Lett.*, vol. 104, no. 4, art. no. 042111, 2014.

[8] A. Herguth, G. Schubert, M. Käs, and G. Hahn, "A new approach to prevent the negative impact of the metastable defect in boron doped CZ silicon solar cells," in *Proc. 4th IEEE World Conf. Photovoltaic Energy Convers.*, 2006, vol. 1, pp. 940–943.

[9] K. Münzer, "Hydrogenated silicon nitride for regeneration of light induced degradation," in *Proc. 24th Eur. Photovoltaic Solar Energy Conf.*, Hamburg, Germany, pp. 1558–1561, 2009.

[10] G. Krugel, W. Wolke, J. Geilker, S. Rein, and R. Preu, "Impact of hydrogen concentration on the regeneration of light induced degradation," *Energy Procedia*, vol. 8, pp. 47–51, 2011.

[11] S. Dubois *et al.*, "The bolid project: Suppression of the boron-oxygen related light-induced-degradation," in *Proc. 27th Eur. Photovoltaic Sol. Energy Conf.*, Frankfurt, Germany, 2012, pp. 749–754.

[12] B. Hallam *et al.*, "Hydrogen passivation of B-O defects in Czochralski silicon," *Energy Procedia*, vol. 38, pp. 561–570, 2013.

[13] S. Wilking, C. Beckh, S. Ebert, A. Herguth, and G. Hahn, "Influence of bound hydrogen states on bo-regeneration kinetics and consequences for high-speed regeneration processes," *Sol. Energy Mater. Sol. Cells*, vol. 131, pp. 2–8, 2014.

[14] C. Sun, F. E. Rougieux, and D. Macdonald, "A unified approach to modelling the charge state of monatomic hydrogen and other defects in crystalline silicon," *J. Appl. Phys.*, vol. 117, no. 4, art. no. 045702, 2015.

[15] M. Gläser and D. Lausch, "Towards a quantitative model for BO regeneration by means of charge state control of hydrogen. *Energy Procedia*, vol. 77, pp. 592–598, 2015.

[16] B. Lim, K. Bothe, and J. Schmidt, "Impact of oxygen on the permanent deactivation of boron–oxygen-related recombination centers in crystalline silicon," *J. Appl. Phys.*, vol. 107, no. 12, art. no. 123707, 2010.

[17] V. Voronkov, R. Falster, B. Lim, and J. Schmidt, "Permanent recovery of electron lifetime in pre-annealed silicon samples: A model based on ostwald ripening," *J. Appl. Phys.*, vol. 112, no. 11, art. no. 113717, 2012.

[18] N. Nampalli, B. Hallam, C. Chan, M. Abbott, and S. Wenham, "Evidence for the role of hydrogen in the stabilization of minority carrier lifetime in boron-doped Czochralski silicon. *Appl. Phys. Lett.*, vol. 106, no. 17, art. no. 173501, 2015.

[19] A. Herguth and G. Hahn, "Kinetics of the boron-oxygen related defect in theory and experiment," *J. Appl. Phys.*, vol. 108, no. 11, art. no. 114509, 2010.

[20] P. Hamer, B. Hallam, M. Abbott, and S. Wenham, "Accelerated formation of the boron-oxygen complex in p-type Czochralski silicon," *Phys. Status Solidi—Rapid Res. Lett.*, vol. 9, no. 5, pp. 297–300, 2015.

[21] B. J. Hallam *et al.*, "Advanced hydrogenation of dislocation clusters and boron-oxygen defects in silicon solar cells," *Energy Procedia*, vol. 77, pp. 799–809, 2015.

[22] T. U. Nærland, H. Angelskår, and E. S. Marstein, "Direct monitoring of minority carrier density during light induced degradation in Czochralski silicon by photoluminescence imaging," *J. Appl. Phys.*, vol. 113, no. 19, art. no. 193707, 2013.

[23] F. Rougieux *et al.*, "Influence of net doping, excess carrier density and annealing on the boron oxygen related defect density in compensated n-type silicon," *J. Appl. Phys.*, vol. 110, art. no. 063708, 2011.

[24] B. Hallam *et al.*, "Advanced bulk defect passivation for silicon solar cells," *IEEE J. Photovoltaics*, vol. 4, no. 1, pp. 88–95, Jan. 2014.

[25] S. Wenham *et al.*, "Advanced hydrogenation of silicon solar cells," Patent WO2013173867 A1, 2013.

[26] P. Hamer *et al.*, "Hydrogen passivation mechanisms in silicon solar cells," in *Proc. 28th Eur. Photovoltaic Sol. Energy Conf.*, Paris, France, pp. 982–987, 2013.

[27] P. Hamer, B. Hallam, S. Wenham, and M. Abbott, "Manipulation of hydrogen charge states for passivation of p-type wafers in photovoltaics," *IEEE J. Photovoltaics*, vol. 4, no. 5, pp. 1252–1260, Sep. 2014.

[28] S. Wilking, A. Herguth, and G. Hahn, "Influence of hydrogen on the regeneration of boron-oxygen related defects in crystalline silicon," *J. Appl. Phys.*, vol. 113, no. 19, art. no. 194503, 2013.

[29] A. Herguth, G. Schubert, M. Käs, and G. Hahn, "Investigations on the long time behavior of the metastable boron– oxygen complex in crystalline silicon," *Prog. Photovoltaics, Res. Appl.*, vol. 16, no. 2, pp. 135–140, 2008.

[30] J. Knobloch *et al.*, "21% efficient solar cells processed from Czochralski grown silicon," in *Proc. 13th Eur. Photovoltaic Sol. Energy Conf.*, 1995, pp. 9–12.

[31] J. Schmidt, A. G. Aberle, and R. Hezel, "Investigation of carrier lifetime instabilities in Cz-grown silicon," in *Proc. 26th IEEE Photovoltaic Spec. Conf.*, 1997, pp. 13–18.

[32] K. Bothe and J. Schmidt, "Electronically activated boron-oxygen-related recombination centers in crystalline silicon," *J. Appl. Phys.*, vol. 99, no. 1, art. no. 013701, 2006.

[33] B. Lim, F. Rougieux, D. Macdonald, K. Bothe, and J. Schmidt, "Generation and annihilation of boron–oxygen-related recombination centers in compensated p-and n-type silicon," *J. Appl. Phys.*, vol. 108, art. no. 103722, 2010.

[34] D. Macdonald, A. Liu, A. Cuevas, B. Lim, and J. Schmidt, "The impact of dopant compensation on the boron–oxygen defect in p-and n-type crystalline silicon," *Phys. Status Solidi (a)*, vol. 208, no. 3, pp. 559–563, 2011.

[35] T. Nærland *et al.*, "Studying light-induced degradation by lifetime decay analysis: Excellent fit to solution of simple second-order rate equation," *IEEE J. Photovoltaics.*, vol. 3, no. 4, pp. 1265–1270, Oct. 2013.

[36] V. V. Voronkov, R. Falster, K. Bothe, and B. Lim, "Light-induced lifetime degradation in boron-doped Czochralski silicon: Are oxygen dimers involved?" *Energy Procedia*, vol. 38, pp. 636–641, 2013.

[37] V. V. Voronkov and R. Falster, "Latent complexes of interstitial boron and oxygen dimers as a reason for degradation of silicon-based solar cells," *J. Appl. Phys.*, vol. 107, no. 5, art. no. 053509, 2010.

[38] S. W. Glunz, S. Rein, W. Warta, J. Knobloch, and W. Wettling, "On the degradation of cz-silicon solar cells," in *Proc. 2nd World Conf. Photovoltaic Sol. Energy Convers.*, Vienna, Austria, 1998, vol. 1, pp. 1343–1346.

[39] R. A. Sinton, A. Cuevas, and M. Stuckings, "Quasi-steady-state photoconductance, a new method for solar cell material and device characterization," in *Proc. 25th IEEE Photovoltaic Spec. Conf.*, 1996, pp. 457–460.

[40] H. Nagel, C. Berge, and A. G. Aberle, "Generalized analysis of quasi-steady-state and quasi-transient measurements of carrier lifetimes in semiconductors," *J. Appl. Phys.*, vol. 86, no. 11, pp. 6218–6221, 1999.

[41] S. Wilking *et al.*, "High speed regeneration of BO-defects: Improving long-term solar cell performance within seconds," in *Proc. 29th Eur. Photovoltaic Sol. Energy Conf. Exhib.*, 2014, pp. 366–372.

Authors' photographs and biographies not available at the time of publication.